

Shock Speed, Cosmic Ray Pressure, and Gas Temperature in the Cygnus Loop

Richard J. Edgar, Greg Salvesen¹, and John C. Raymond

Smithsonian Astrophysical Observatory

¹also University of Michigan

Abstract:

We have measured proper motions (from two epochs of Palomar Observatory Sky Survey plates) and post-shock temperatures (from ROSAT pointed observations) for 18 positions around the forward shock in the Cygnus Loop. The differences between shock velocity derived from the two methods constrain the efficiency of cosmic ray acceleration.

Our measurements show a ratio of cosmic ray pressure to gas pressure consistent with zero. In some cases, our formal upper limits are negative. This suggests that the distance to the Cygnus Loop may be underestimated, the electron temperatures are lower than measured with ROSAT, or an additional source of heating for the electrons is present.

We acknowledge support from NASA contract NAS8-03060 with the Chandra X-ray Center, an NSF Research Experiences for Undergraduates (REU) award, Department of Defense Awards to Stimulate and Support Undergraduate Research Experiences (ASSURE) grant number 0754568, and by the Smithsonian Institution.

The Idea

- We measure the proper motion for the Balmer dominated filaments at a number of points (as marked) around the rim of the Cygnus loop.
- This proper motion combined with a distance estimate gives the shock speed.
- The electron temperature of the post-shock gas is measured by fitting the ROSAT x-ray spectrum.

$$\frac{P_{CR}}{P_G} = \frac{3mv_s^2}{16kT_s} - 1$$

- Any leftover energy can go into accelerating cosmic rays.
- **But...** the electrons are too hot for the measured proper motion, given the best available distance.
- As can be seen in Figure 3, the formal limits on this pressure ratio are often negative.

Proper Motions

- The Palomar Observatory Sky Survey (POSS) took red plates of the Cygnus Loop region at two epochs, separated by about 39.1 years. The H- α filaments are clearly visible, and obviously moved.
- The data were rotated, and regions free of stars were selected (see Figure 1 for filament 7). Autocorrelations were performed, and highly significant proper motions were derived.
- Errors were estimated using bootstrap resampling methods.

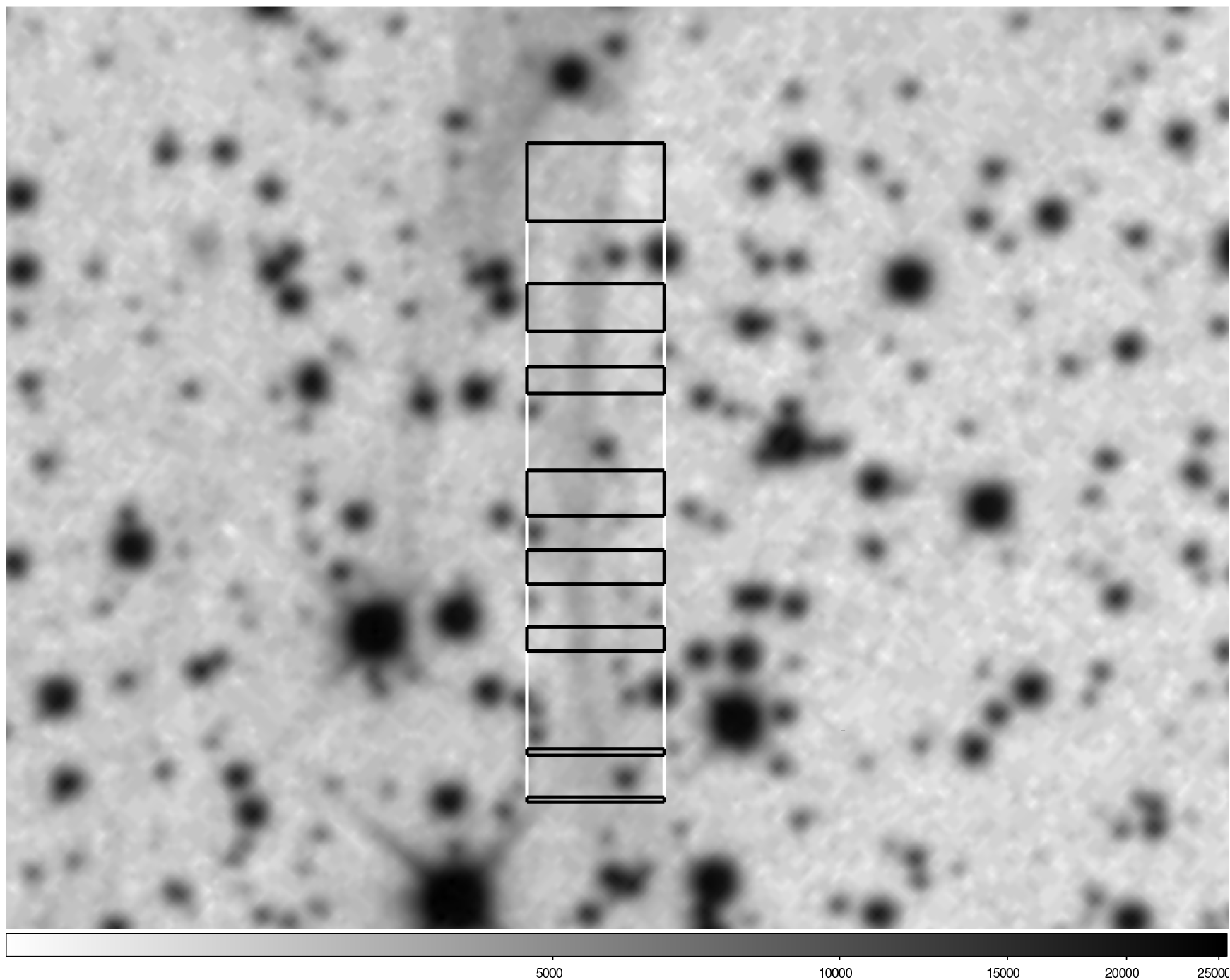


Figure 1: Region selection process for H- α Filament 7. Note exclusion of the stars.

Post-shock Temperatures

- Data from ROSAT PSPC pointed observations were extracted for regions from 25'' to 100'' behind each filament.
- These were fitted to a variety of one- and two-temperature models. A low temperature component with $kT \sim 135$ eV is ubiquitous. Similar results are found from fitting the observations of the forward shock regions with Suzaku, XMM, and Chandra.

Distance

- We take our distance estimate from Blair, Sankrit, Torres, Chayer and Danforth, 2009, ApJ, 692, 335.
- Blair et al. observed subdwarf OB (sdOB) star KPD 2055+3111 with FUSE and found a broad $\lambda 1032$ O VI absorption line in its spectrum. This demonstrates that the star is behind the Cygnus Loop.
- From optical spectroscopy, the distance to the star is 576 ± 61 pc. We take this to be an upper limit to the distance to the Cygnus Loop.

Conclusions

- Combining fitted temperatures with shock velocities from proper motions and the distance of Blair et al (derived from high velocity UV absorption lines toward a subdwarf O star behind the remnant), we find upper limits to the P_{CR}/P_G ratio which are often negative.
- It seems clear from these results that P_{CR}/P_G is small, and that the forward shock in the Cygnus Loop is not a highly efficient accelerator of cosmic rays.
- Clearly negative values of P_{CR}/P_G are unphysical.
- Possible outs:
 - Electron temperatures are higher than we measure with ROSAT (but Suzaku, Chandra, XMM get similar low temperature results)
 - Distance is larger; ~ 900 pc (but what about the Blair et al. sdOB star?)
 - Sharp density gradient (why all around the loop right now, when the loop is non-spherical?)
Reflected shock (same objections).
 - Thermal conduction up to the shock front from the hot interior?

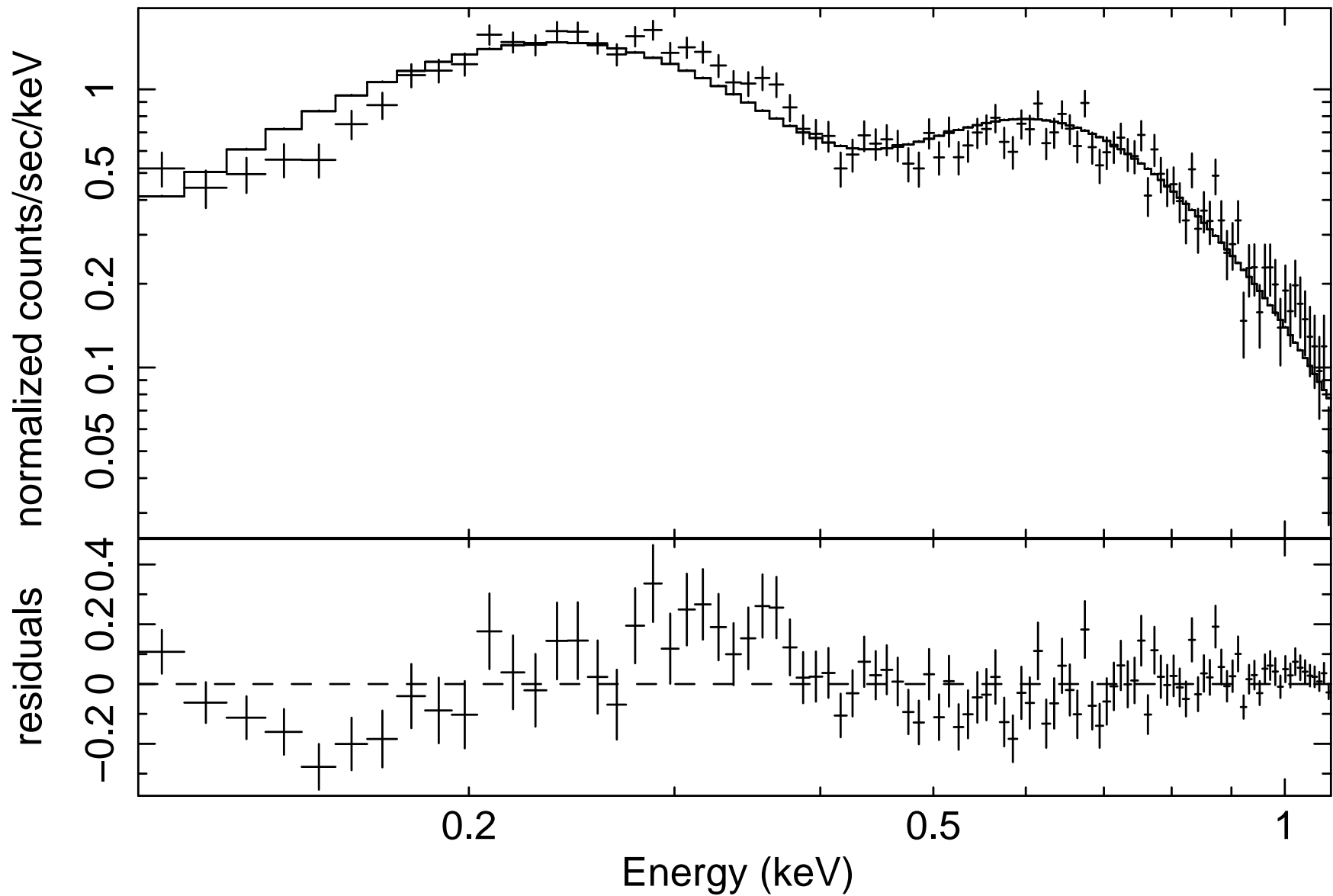


Figure 2: Fit of apec single-temperature model to ROSAT data for Filament 7.

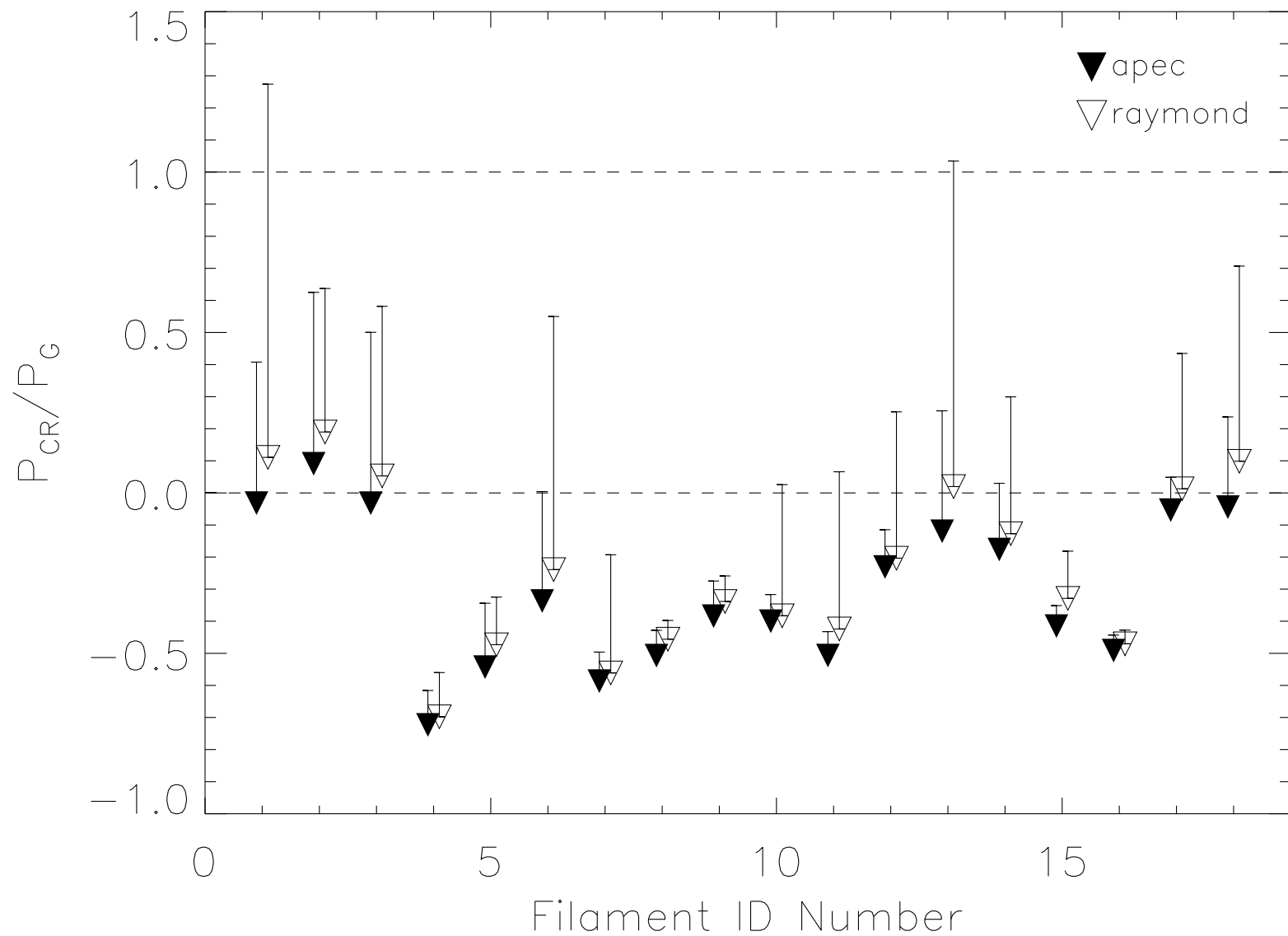


Figure 3: Upper limits to the cosmic ray to gas pressure ratio, given temperatures fit using `apec` and `raymond` models.

Table 1:

Proper Motion and P_{cr}/P_g Values for Selected H α Filaments

| Filament ID | α_{J2000} | δ_{J2000} | Proper Motion arcsec / 39.1 yr | v_{max} km s $^{-1}$ | $(P_{CR}/P_G)_{apec}$ | $(P_{CR}/P_G)_{apec}^{MAX}$ | d_{apec}^{MIN} pc | $(P_{CR}/P_G)_{raymond}$ | $(P_{CR}/P_G)_{raymond}^{MAX}$ | $d_{raymond}^{MIN}$ pc |
|-------------|------------------|------------------|-----------------------------------|---------------------------|-----------------------|-----------------------------|------------------------|--------------------------|--------------------------------|---------------------------|
| 1 | 20 51 23.9 | 32 24 22.5 | 5''1 \pm 0''2 | 403 | -0.032 | 0.408 | 537 | 0.111 | 1.274 | 422 |
| 2 | 20 51 29.9 | 32 24 21.8 | 5''4 \pm 0''2 | 433 | 0.091 | 0.625 | 500 | 0.190 | 0.637 | 498 |
| 3 | 20 51 38.6 | 32 24 14.5 | 5''2 \pm 0''2 | 416 | -0.032 | 0.501 | 520 | 0.053 | 0.582 | 507 |
| 4 | 20 54 13.1 | 32 21 14.0 | 2''7 \pm 0''2 | 225 | -0.723 | -0.616 | 1028 | -0.698 | -0.560 | 960 |
| 5 | 20 54 26.2 | 32 19 36.5 | 3''4 \pm 0''2 | 278 | -0.543 | -0.344 | 786 | -0.473 | -0.325 | 775 |
| 6 | 20 54 43.4 | 32 16 04.0 | 4''1 \pm 0''2 | 333 | -0.337 | -0.004 | 638 | -0.239 | 0.550 | 512 |
| 7 | 20 55 06.3 | 32 10 03.8 | 3''0 \pm 0''1 | 240 | -0.587 | -0.496 | 897 | -0.561 | -0.193 | 709 |
| 8 | 20 55 14.7 | 32 07 38.9 | 3''4 \pm 0''1 | 274 | -0.507 | -0.428 | 843 | -0.456 | -0.397 | 821 |
| 9 | 20 55 18.9 | 32 06 58.0 | 3''7 \pm 0''1 | 294 | -0.384 | -0.275 | 748 | -0.338 | -0.259 | 740 |
| 10 | 20 55 34.6 | 32 01 40.2 | 3''5 \pm 0''1 | 279 | -0.400 | -0.317 | 771 | -0.383 | 0.026 | 629 |
| 11 | 20 55 44.9 | 31 59 43.8 | 3''1 \pm 0''2 | 254 | -0.507 | -0.432 | 845 | -0.424 | 0.066 | 617 |
| 12 | 20 55 51.8 | 31 57 34.8 | 4''0 \pm 0''2 | 319 | -0.231 | -0.115 | 677 | -0.203 | 0.253 | 569 |
| 13 | 20 55 56.5 | 31 55 55.1 | 4''2 \pm 0''7 | 375 | -0.120 | 0.256 | 568 | 0.020 | 1.034 | 447 |
| 14 | 20 57 20.2 | 31 37 32.4 | 4''3 \pm 0''1 | 342 | -0.176 | 0.030 | 628 | -0.127 | 0.299 | 559 |
| 15 | 20 45 11.9 | 31 03 50.0 | 3''4 \pm 0''1 | 272 | -0.415 | -0.351 | 791 | -0.329 | -0.182 | 704 |
| 16 | 20 45 15.3 | 31 01 41.4 | 3''3 \pm 0''1 | 264 | -0.492 | -0.443 | 854 | -0.470 | -0.428 | 842 |
| 17 | 20 56 37.4 | 30 08 34.4 | 4''5 \pm 0''1 | 358 | -0.054 | 0.049 | 622 | 0.013 | 0.434 | 532 |
| 18 | 20 56 34.8 | 30 06 27.8 | 4''8 \pm 0''1 | 379 | -0.044 | 0.237 | 573 | 0.099 | 0.707 | ... |

The coordinates listed represent the right ascension and declination at the center of the extracted filament. The measured proper motions are derived from comparing POSS-I and POSS-II images observed 39.1 years apart. Errors on proper motion do not include a $\leq 0''.1$ uncertainty from image alignment. Shock speed, v_s , is calculated from the product of proper motion and distance using the upper limits of proper motion + uncertainty and $576+61 = 637$ pc (Blair et al. 2009). All cosmic ray to gas pressure ratio calculations are based on these conservative upper limits. Minimum distances to the Cygnus Loop based on our measurements assume $P_{CR}/P_G = 0$ with an upper limit on proper motion and lower limit on temperature. We compare results from individual X-ray temperature fits with the XSPEC models `apec` and `raymond`.

Table 2:

X-ray Spectral Fit Parameters with the `apec` Model

| Filament ID | T_{cos} eV | $N_{\text{H},\text{cos}}$ 10^{20} cm^{-2} | $(\chi^2/\nu)_{\text{cos}}$ | T_{dep} eV | $(\chi^2/\nu)_{\text{dep}}$ | T_{low} eV | T_{high} eV | $(\chi^2/\nu)_{\text{double}}$ |
|-------------|------------------------|--|-----------------------------|------------------------|-----------------------------|------------------------|-------------------------|--------------------------------|
| 1 | 187_{-6}^{+6} | $2.4_{-0.2}^{+0.2}$ | 1.65 | 162_{-7}^{+10} | 3.37 | 137 | 536 | 1.13 |
| 2 | 192_{-6}^{+7} | $2.4_{-0.2}^{+0.2}$ | 1.80 | 198_{-9}^{+10} | 3.01 | 137 | 602 | 1.28 |
| 3 | 198_{-6}^{+7} | $2.5_{-0.2}^{+0.2}$ | 1.44 | 230_{-10}^{+10} | 2.47 | 137 | 336 | 1.16 |
| 4 | 190_{-6}^{+6} | $2.3_{-0.2}^{+0.2}$ | 0.96 | 194_{-8}^{+9} | 1.86 | 157 | 454 | 0.85 |
| 5 | 181_{-4}^{+5} | $2.5_{-0.2}^{+0.2}$ | 1.48 | 159_{-6}^{+8} | 3.21 | 140 | 605 | 1.06 |
| 6 | 179_{-2}^{+4} | $2.1_{-0.1}^{+0.1}$ | 2.33 | 151 | 5.75 | 132 | 380 | 1.60 |
| 7 | 154_{-4}^{+5} | $2.6_{-0.2}^{+0.2}$ | 2.22 | 119 | 5.95 | 136 | 541 | 1.53 |
| 8 | 170_{-4}^{+12} | 1.2 | 1.26 | 118_{-4}^{+4} | 3.44 | 156 | 661 | 1.06 |
| 9 | 159_{-5}^{+6} | $1.7_{-0.2}^{+0.2}$ | 1.45 | 115_{-4}^{+4} | 3.63 | 141 | 656 | 1.14 |
| 10 | 146 | 2.1 | 5.59 | 80.8 | 10.7 | 135 | ... | 3.90 |
| 11 | 139 | 1.9 | 5.07 | 80.8 | 9.92 | 135 | 690 | 3.95 |
| 12 | 145_{-3}^{+3} | $1.1_{-0.1}^{+0.1}$ | 2.91 | 80.8 | 7.18 | 136 | 685 | 1.55 |
| 13 | 139 | 1.7 | 5.03 | 80.8 | 9.34 | 133 | 863 | 3.40 |
| 14 | 159_{-7}^{+8} | $1.8_{-0.3}^{+0.3}$ | 1.48 | 115_{-4}^{+7} | 3.14 | 135 | 727 | 0.89 |
| 15 | 140_{-5}^{+3} | $2.1_{-0.2}^{+0.2}$ | 2.81 | 80.8 | 5.24 | 135 | 812 | 2.29 |
| 16 | 150_{-4}^{+4} | $2.4_{-0.1}^{+0.1}$ | 1.02 | 86.8 | 1.91 | 148 | 692 | 1.03 |
| 17 | 152_{-9}^{+13} | $4.2_{-0.7}^{+0.6}$ | 1.19 | 146_{-7}^{+9} | 1.91 | 145 | 159 | 1.24 |
| 18 | 169_{-20}^{+11} | $3.8_{-0.5}^{+1.1}$ | 1.32 | 155_{-10}^{+23} | 1.88 | 138 | 633 | 1.24 |

ROSAT PSPC X-ray spectral parameters corresponding to fits behind each filament with the XSPEC model `apec`. The subscript 'cos' refers to single-temperature model fits `phabs` \times `apec` with abundances fixed to cosmic. The subscript 'dep' refers to single-temperature model fits `phabs` \times `vappec` with depleted abundances fixed to 10% cosmic. The subscript 'double' refers to double-temperature model fits `phabs` \times (`apec+apec`) with abundances fixed to cosmic. We allowed N_H to vary from an initial value of $1.5 \times 10^{20} \text{ cm}^{-2}$. We stress that the errors listed in the table are generated in XSPEC and are not representative of actual uncertainties based on the variation in best fit values when comparing similar models. Fits with no errors or parameters listed are unphysical or limited by χ^2 statistics.